

Mechanism of action of hepatitis B virus S antigen transport-inhibiting oligonucleotide polymer, STOPS, molecules

C. Cheng Kao,¹ Yuchun Nie,¹ Suping Ren,¹ N. Tilani T.S. De Costa,¹ Rajendra K. Pandey,¹ Jin Hong,¹ David B. Smith,¹ Julian A. Symons,¹ Leonid Beigelman,¹ and Lawrence M. Blatt¹

¹Aligos Therapeutics, Inc., 1 Corporate Drive, South San Francisco, CA 94080, USA

A functional cure of chronic hepatitis B requires eliminating the hepatitis B virus (HBV)-encoded surface antigen (HBsAg), which can suppress immune responses. STOPS are phosphorothioated single-stranded oligonucleotides containing novel chemistries that significantly reduce HBsAg produced by HBV-infected liver cells. The STOPS molecule ALG-10000 functions inside cells to reduce the levels of multiple HBV-encoded molecules. However, it does not bind HBV molecules. An affinity resin coupled with ALG-10000 was found to bind several proteins from liver cells harboring replicating HBV. Silencing RNAs targeting host factors SRSF1, HNRNPA2B1, GRP78 (HspA5), RPLP1, and RPLP2 reduced HBsAg levels and other HBV molecules that are concomitantly reduced by STOPS. Host proteins RPLP1/RPLP2 and GRP78 function in the translation of membrane proteins, protein folding, and degradation. ALG-10000 and the knockdowns of RPLP1/2 and GRP78 decreased the levels of HBsAg and increased their ubiquitination and proteasome degradation. GRP78, RPLP1, and RPLP2 affected HBsAg production only when HBsAg was expressed with HBV regulatory sequences, suggesting that HBV has evolved to engage with these STOPS-interacting molecules. The STOPS inhibition of HBsAg levels in HBV-infected cells occurs by sequestering cellular proteins needed for proper expression and folding of HBsAg.

INTRODUCTION

Despite the availability of a highly effective vaccine, over 296 million people worldwide were living with chronic hepatitis B (CHB) in 2019.¹ Untreated CHB can result in a lifetime of illness. Up to 40% of the patients will progress to liver cirrhosis and severe diseases.²

Persistent HBV infection is the result of the patient's immune system failing to clear the virus infection. HBV produces various molecules during infection that can suppress innate and adaptive immunity, including the HBV surface (S) antigen (HBsAg).^{3,4} To increase the challenge to cure, HBV produces low copy numbers of covalently closed circular DNAs (cccDNAs) in the nucleus of the infected hepatocytes and can integrate partial forms of its genome into human chromosomes. Current classes of approved therapeutics for CHB, re-

combinant interferons and nucleos(t)ide analogues, are highly effective in controlling virion production but have low cure rates either separately or in combination.^{5,6,9-11}

The difficulty of eradicating HBV has led to the concept of functional cure, the elimination of virus production and the clearance of immunosuppressive HBV molecules, especially HBsAg.⁶ Some patients with prolonged HBsAg loss seroconverted and displayed improved clinical outcomes for years, even though HBV DNA persisted in their livers.⁷⁻¹⁰

Numerous direct-acting antivirals targeting HBV entry, capsid assembly, cccDNA, HBV RNA, and HBsAg secretion are in development, with a goal toward a functional cure.^{10,12} Nucleic acid polymers (NAPs), which are phosphorothioate-containing oligonucleotides, are a promising class of therapeutics for treating CHB. NAPs can prevent the establishment of duck hepatitis virus infection and the release of the duck HBsAg from infected cells.¹³⁻¹⁵ In clinical trials, a significant proportion of patients treated with NAPs had more than a 5-log₁₀ IU/mL decrease of HBsAg in their plasma 5 weeks or more after treatment onset.^{16,17} Some of the patients exhibiting seroclearance produced antibodies to HBsAg.¹⁷

How NAPs function to inhibit HBV infection and reduce HBsAg is not clear. In cultured cells, NAPs do not appear to activate innate immune responses.¹⁸ NAPs could also inhibit the hepatitis delta virus, a subviral agent that co-infects hepatocytes with HBV and uses the HBsAg to form infectious particles.¹⁹ Notably, NAPs do not demonstrate efficacy in animal models of HBV infection and efficacy was limited to human CHB patients.

We have developed a new class of NAPs called S-antigen transport-inhibiting oligonucleotide polymers (STOPS). STOPS can potentially inhibit HBV infection and HBsAg production *in vitro*.^{20,21} Here, we

Received 21 May 2021; accepted 9 December 2021;
<https://doi.org/10.1016/j.omtn.2021.12.013>.

Correspondence: C. Cheng Kao, Aligos Therapeutics, Inc., 1 Corporate Drive, South San Francisco, CA 94080, USA.

E-mail: chekao@gmail.com



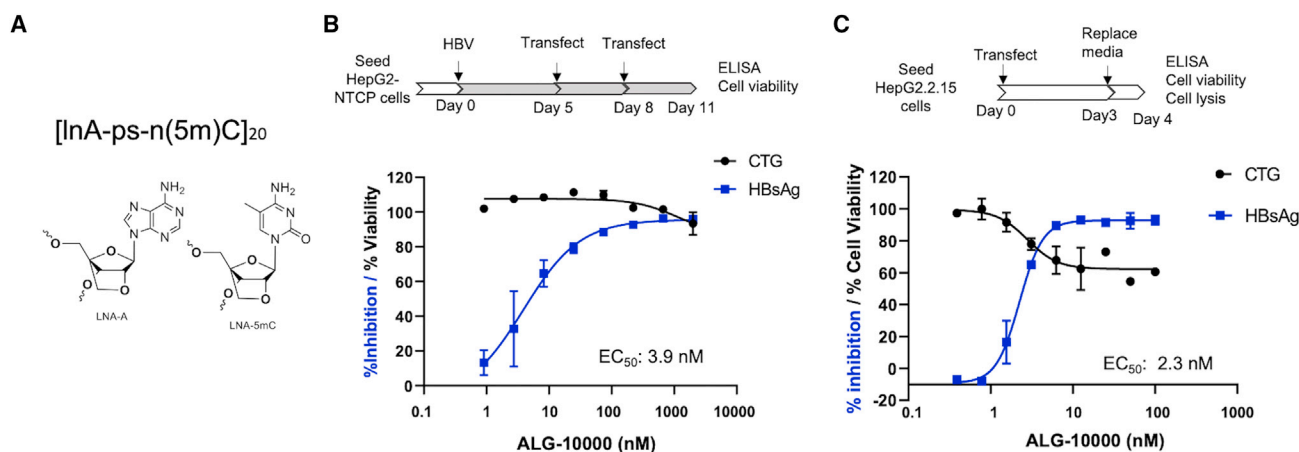


Figure 1. ALG-10000, a prototype STOPS molecule

(A) The chemical structure of ALG-10000. InA denotes an LNA nucleotide of adenosine. ps denotes a phosphorothioate. In(5m)C denotes an LNA 5-methylcytosine. (B) ALG-10000 can inhibit HBV infection of HepG2 cells expressing the HBV entry receptor NTCP. The schematic details the protocol used. The dose-response curve for the inhibition of extracellular HBsAg is shown in blue, while the effect on cell viability is shown in black. Each error bar represents one standard deviation of uncertainty. (C) ALG-10000 can reduce extracellular HBsAg produced by the integrated HBV genome in HepG2.2.15 cells. The dose response for inhibition of extracellular HBsAg is shown in blue, and the effect on cell viability is shown in black. Each error bar represents one standard deviation of uncertainty.

describe the elucidation of the mechanism of action of a STOPS molecule in inhibiting HBV infection and reducing HBsAg levels.

RESULTS

STOPS molecule ALG-10000 can potently reduce extracellular HBsAg produced by HBV

ALG-10000 consists of 20 repeats of adenosine and 5-methyl-cytosine locked nucleic acid (LNA) nucleosides connected by phosphorothioate linkages (Figure 1A). In cultured HepG2 cells expressing the HBV entry receptor, sodium taurocholate co-transporting polypeptide (NTCP), ALG-10000 reduced extracellular HBsAg encoded by HBV in a concentration-dependent manner (Figure 1B). During an infection, extracellular HBsAg is a combination of secreted HBsAg oligomers and the envelope proteins on hepatitis B virions. The effective concentration for a 50% reduction of extracellular HBsAg (EC_{50}) was 4 nM and the cellular cytotoxicity at 50% (CC_{50}) was greater than 1 μ M. In HepG2.2.15 cells that possess an integrated, tandem copy of the HBV genome, ALG-10000 reduced extracellular HBsAg levels with an EC_{50} of 3 nM and a CC_{50} of over 100 nM, the highest concentration tested (Figure 1C). STOPS can reduce extracellular HBsAg levels in HepG2.2.15 cells at better than 20-fold lower concentrations than can NAPs.²⁰

Properties of STOPS in reducing HBV infection

HepG2.2.15 cells were used as a model system to understand how STOPS affect HBV replication and virion production. Initial key findings included that transfection of ALG-10000 into cells is required to reduce HBsAg levels. Post transfection, ALG-10000 localizes primarily to the cell cytoplasm but does not extensively co-localize with HBsAg. Furthermore, ALG-10000 does not activate nucleic acid-

sensing innate immune receptors. These results are detailed in Figure S1.

We seek to understand the kinetics of HBsAg reduction in HepG2.2.15 cells treated with STOPS. ALG-10000 was transfected into the cells and the medium collected every 12 h. The amount of HBsAg in the medium was quantified and normalized to that of mock-treated control cells. The inhibition of extracellular HBsAg by ALG-10000 occurred in a biphasic manner that reached maximal levels about 72 h after the introduction of ALG-10000 (Figure 2A). The biphasic reduction of HBsAg suggests that ALG-10000 has a complex mechanism to inhibit extracellular HBsAg.

The reduced extracellular HBsAg could be solely due to ALG-10000 inhibiting HBsAg transport. In this case, ALG-10000 will not reduce the intracellular HBsAg level and may even increase it due to intracellular accumulation. To examine this, cell-associated HBsAg levels were assessed by western blots. Intracellular HBsAg was reduced in cells transfected with ALG-10000, and the reduction was more pronounced after 72 h (Figures 2B and S2A). The reduction of intracellular HBsAg suggest that ALG-10000 acts on a process or processes that precede the transport and trafficking of the HBsAg into the extracellular media.

We examined whether STOPS would inhibit HBV molecules in addition to HBsAg. Secreted HBV E antigen (HBeAg) was reduced after transfection of ALG-10000 (Figure 2C). The EC_{50} for HBeAg reduction was 2 nM, but the greatest extent of HBeAg inhibition (~75%) was reproducibly lower than that of HBsAg (>90%). The HBV polymerase was reduced by ALG-10000 (Figure 2D). Intracellular HBV core levels were also reduced but at a more modest level compared

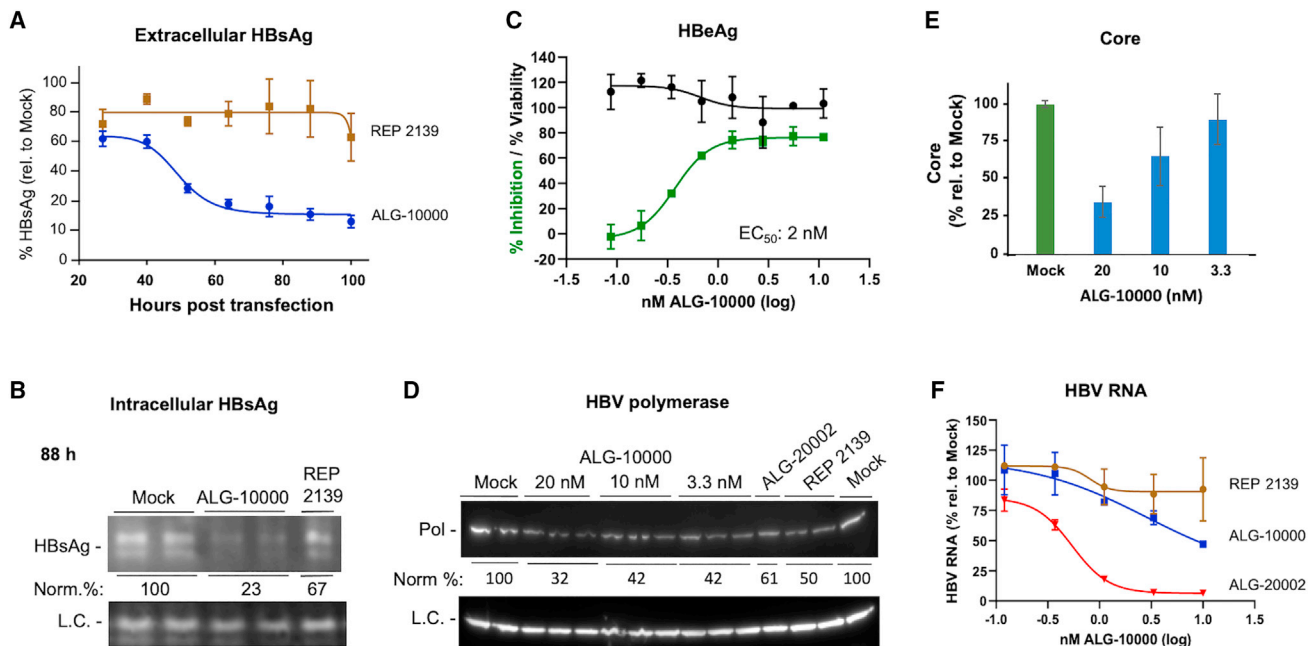


Figure 2. Properties of ALG-1000 inhibition of HBV replication

(A) Kinetics of the inhibition of extracellular HBsAg by ALG-10000 and REP 2139. Each of the data points represents the HBsAg amount present in the HepG2.2.15 cell culture medium over a 12-h period. The amount is normalized to the levels in the mock-transfected cells. ALG-10000 was transfected into cells at 8 nM and REP 2139 at 20 nM. (B) Western blot image showing that ALG-10000 reduces intracellular large S antigen in HepG2.2.15 cells. L.C. denotes a loading control. (C) Dose response for the inhibition of HBeAg production by HepG2.2.15 cells. HBeAg cell viability shown in green and cell viability in black. (D) Western blot image showing that ALG-10000 can inhibit HBV polymerase accumulation. ALG-20002 was transfected at 5 nM. REP 2139 was transfected at 40 nM. The LC is the cellular GAPDH protein. (E) ALG-10000 can inhibit the accumulation of the HBV core in a concentration-dependent manner. (F) ALG-10000 can modestly reduce the accumulation of total HBV RNA present in the cell. HBV RNAs present in the cell lysate 72 h after transfection were quantified by detection of the HBx sequence found in all HBV RNAs. ALG-20002 is an antisense oligonucleotide that directly targets HBV RNA sequences for degradation. In the graphs in panel A, C, and F, each error bar represents one standard deviation of uncertainty.

with those of the HBsAg and HBeAg (Figure 2E). Finally, total HBV RNA in ALG-10000-treated cells was found to be reduced by only up to 50% (Figure 2F). Notably, an antisense oligonucleotide ALG-20002, which targets a sequence downstream of the HBsAg open reading frame (ORF), reduced the total HBV RNA to less than 5% (Figure 2F). ALG-10000 thus reduced the amounts of multiple HBV proteins and RNA; however, the levels of reduction differed. These differences suggest that STOPS use a complex mechanism to inhibit HBV protein and nucleic acid production.

ALG-10000 binds host factors needed for HBsAg production

STOPS could exert their inhibitory effect on HBV infection by binding one or more host factors required to produce HBV molecules. To identify these host proteins, we generated an ALG-10000 affinity resin and incubated it with solubilized extracts from HepG2.2.15 cells. After several stringent washes, proteins that remained bound were digested with trypsin and subjected to liquid chromatography-tandem mass spectrometry (LC-MS/MS) and assignment to proteins. All proteins assigned with high confidence are derived from the host cell (Figure 3A); no HBV proteins were detected.

To confirm that the proteins that bind to ALG-10000 have a role in HBV infection, small interfering RNAs (siRNAs) were used to knock

down the host mRNA/protein and the amount of extracellular HBsAg produced by HepG2.2.15 cells was determined. Four of the siRNAs targeting host proteins potently reduced the amount of extracellular HBsAg, each with an EC_{50} of less than 2 nM (Figure 3B). The siRNAs demonstrated no apparent cytotoxicity, even at the highest concentrations tested (Figures 3B and S3). siRNAs that target other proteins pulled down by ALG-10000 either had no effect on HBsAg levels or reduced HBsAg by less than 25%.

The four siRNAs targeted GRP78/HSP5A (glucose-regulated protein 78; heat shock protein family A (Hsp70) member 5), RPLP2 (ribosomal protein lateral stalk subunit P2), SRSF1 (serine-arginine splicing factor 1), and HNRNPA2B1 (heterogeneous ribonucleoprotein A2B1). RPLP2 functions in translating select membrane proteins.²² GRP78 is a chaperone for membrane-associated proteins and a regulator of the unfolded protein response.²³ SRSF1 and HNRNPA2B1 participate in RNA processing, although they also have roles in other nucleic acid-associated processes.^{22,23,25} All four proteins have previously been described to function in viral infection.^{26–30}

RPLP2 forms a heterodimer with RPLP1 that is attached to the ribosome through RPLP0.^{26,31} Our proteomic analysis did not identify

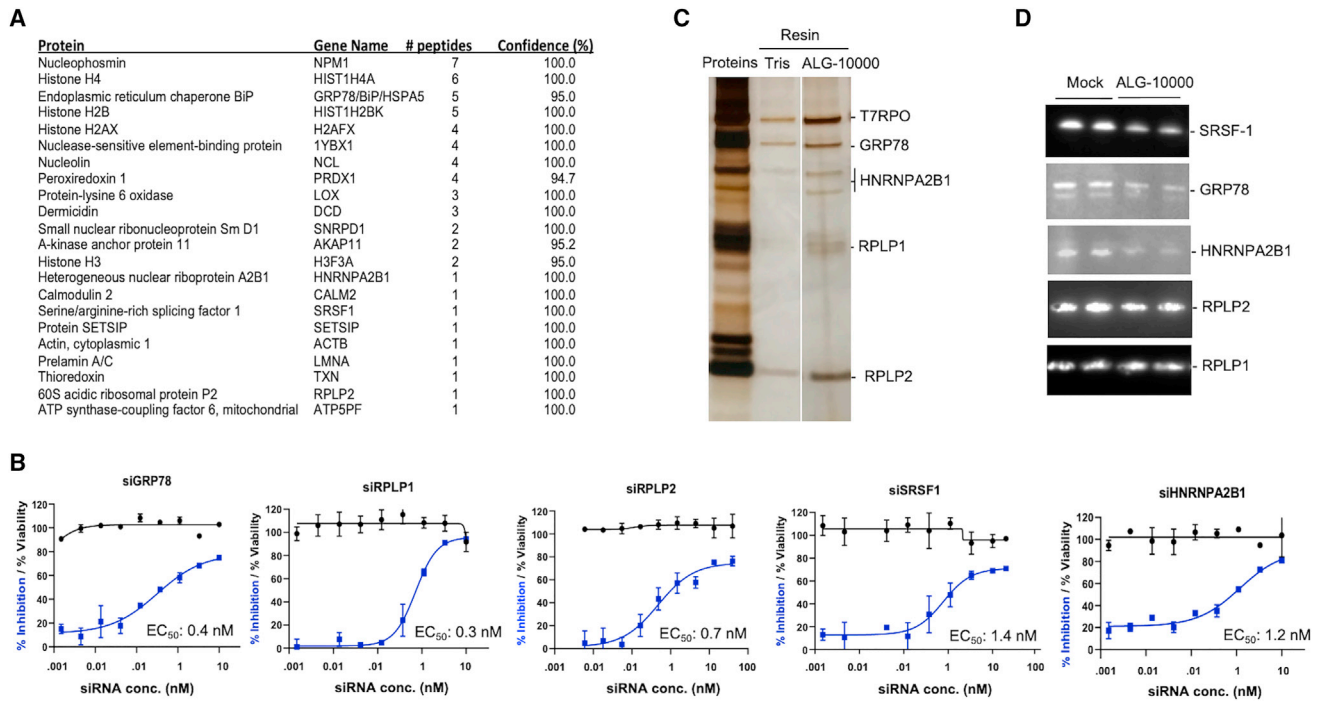


Figure 3. Five host proteins that bind ALG-10000 affect extracellular HBsAg levels

(A) Partial list of proteins that bind ALG-10000 affinity column. The proteins listed are identified with high confidence. (B) Dose responses for the inhibition of extracellular HBsAg levels and effects on cell viability by siRNA knockdowns of the host factors. Each error bar represents one standard deviation of uncertainty. (C) Recombinant proteins of RPLP1, RPLP2, GRP78, and HNRNPA2B1 can bind ALG-10000. The image is of a silver-stained polyacrylamide gel. The lane labeled “Proteins” contains the input proteins present in the analysis. The lane labeled “Tris” shows the amounts of the proteins pulled down by the affinity resin that lacks ALG-10000. (D) ALG-10000 can decrease the abundance of three of the cellular proteins that interact with ALG-10000. The image is from a western blot analysis of lysates from HepG2.2.15 cells that were transfected with 8 nM ALG-10000 and harvested 76 h after transfection.

RPLP1. However, an siRNA that knocks down RPLP1 effectively reduced HBsAg levels with an EC_{50} of less than 2 nM (Figure 3B). Furthermore, a recombinant RPLP1 protein binds to the ALG-10000 affinity resin, although less well than recombinant RPLP2 (Figure 3C). The knockdowns of RPLP1 and RPLP2 resulted in a similar inhibition of HBsAg, suggesting that these proteins function in HBsAg production. RPLP1 is, therefore, the fifth host factor that binds ALG-10000 and contributes to the normal levels of extracellular HBsAg.

We sought to confirm the functional relevance of the identified host proteins. Recombinant proteins GRP78 and HNRNPA2B1 were found to bind to the ALG-10000 affinity resin (Figure 3C). In addition, the amounts of SRSF1, GRP78, and HNRNPA2B1 were reduced in cells transfected with ALG-10000 for 76 h (Figures 3D and S4). The levels of RPLP1 and RPLP2 were less affected by ALG-10000 at this time point (Figure 3D). However, their abundances were more obviously reduced in cells transfected with ALG-10000 for more than 76 h (data not shown). ALG-10000 may render bound proteins more susceptible to degradation.

We have further validated a role for GRP78 in HBV HBsAg production. GRP78 can function with a co-chaperone DNAJB9. siRNA

knockdown of DNAJB9 decreased HBsAg levels (Figure S5A). In addition, deoxynivalenol, an inhibitor of GRP78, was found to reduce HBsAg levels (Figures S5B and S5C). Altogether these results confirm that GRP78, RPLP1, RPLP2, SRSF1, and HNRNPA1B2 interact with ALG-10000 and function in extracellular HBsAg production.

STOPS optimally reduce HBsAg by binding to multiple host factors

STOPS could bind to multiple cellular factors through a combination of their sequence, length, and/or higher-order structures. Truncating STOPS to be less than 32 nt in length was shown to severely decrease HBsAg production inhibition.²⁰ To examine whether STOPS molecules possess secondary or tertiary structures, we examined whether ALG-10000 exhibits the hyperchromicity effect, an increase in absorbance upon denaturation. ALG-10000 absorbance was only negligibly affected by temperature, suggesting that it lacks base-pairing interactions and exists as a largely unstructured polymer (Figure 4A). The AC repeats in STOPS and the phosphorothioate backbone are likely significant features recognized by cellular proteins.

Altering the STOPS sequence should affect the proteins that it binds. To test this, we made STOPS molecules that contain one or more motifs that are more specifically recognized by SRSF1 and HNRNPA2B1.

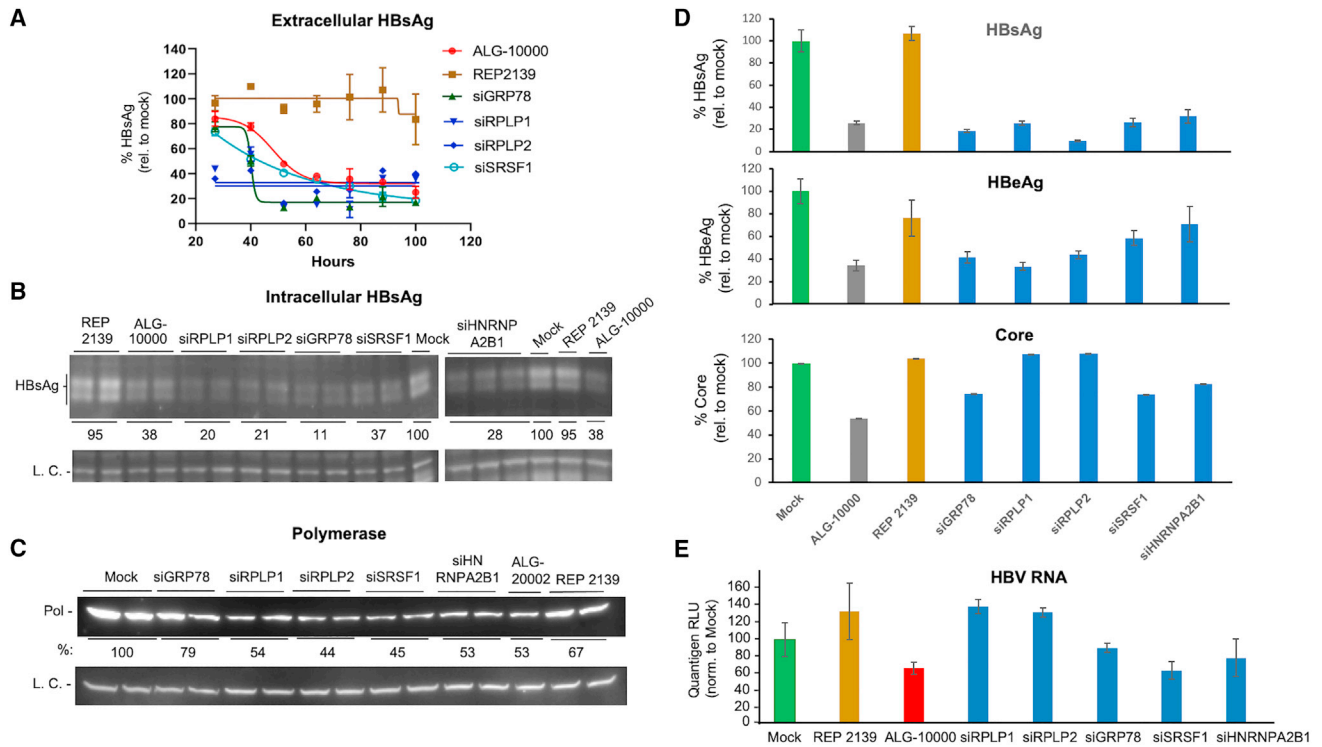


Figure 5. The five host factors affect the abundance of multiple HBV molecules

(A) Kinetics of the decrease in extracellular HBsAg produced by HepG2.2.15 cells transfected with siRNAs. The amount of HBsAg produced was measured in 12-h intervals after siRNA transfection and normalized to the level produced by mock-treated cells. The siRNAs were transfected at a final concentration of 10 nM. REP 2139 was at 20 nM. (B) siRNAs that knock down the five host factors reduced the levels of intracellular HBsAg. The western blot image contains the signal for the large S antigen. The LC is of the β -actin protein. The knockdown of the host factors is shown in Figure S3. (C) The five host factor siRNAs can reduce the HBV polymerase levels. The western blot image shows the amounts of the HBV polymerase identified by a monoclonal antibody specific to the HBV polymerase. The L.C. shows the amount of β -actin protein. Additional western blots of cellular proteins are shown in Figure S6. HepG2.2.15 cells were transfected with a final concentration of 10 nM siRNA, 5 nM ALG-20002, 8 nM ALG-10000, or 20 nM REP 2139. (D) The host factors have differential effects on the amounts of HBsAg, HBeAg, and core. ALG-10000 was transfected into HepG2.2.15 cells at 8 nM and the siRNAs at 10 nM. (E) Total HBV RNAs are modestly reduced by the knockdown of SRSF1 and HNRNP A2B1, but not by knockdown of RPLP1 or RPLP2. The cells were harvested 76 h after transfection. The amount of HBV RNA was normalized to the amount of GAPDH in the cells. In the graphs on panel A and D, each error bar represents one standard deviation of uncertainty.

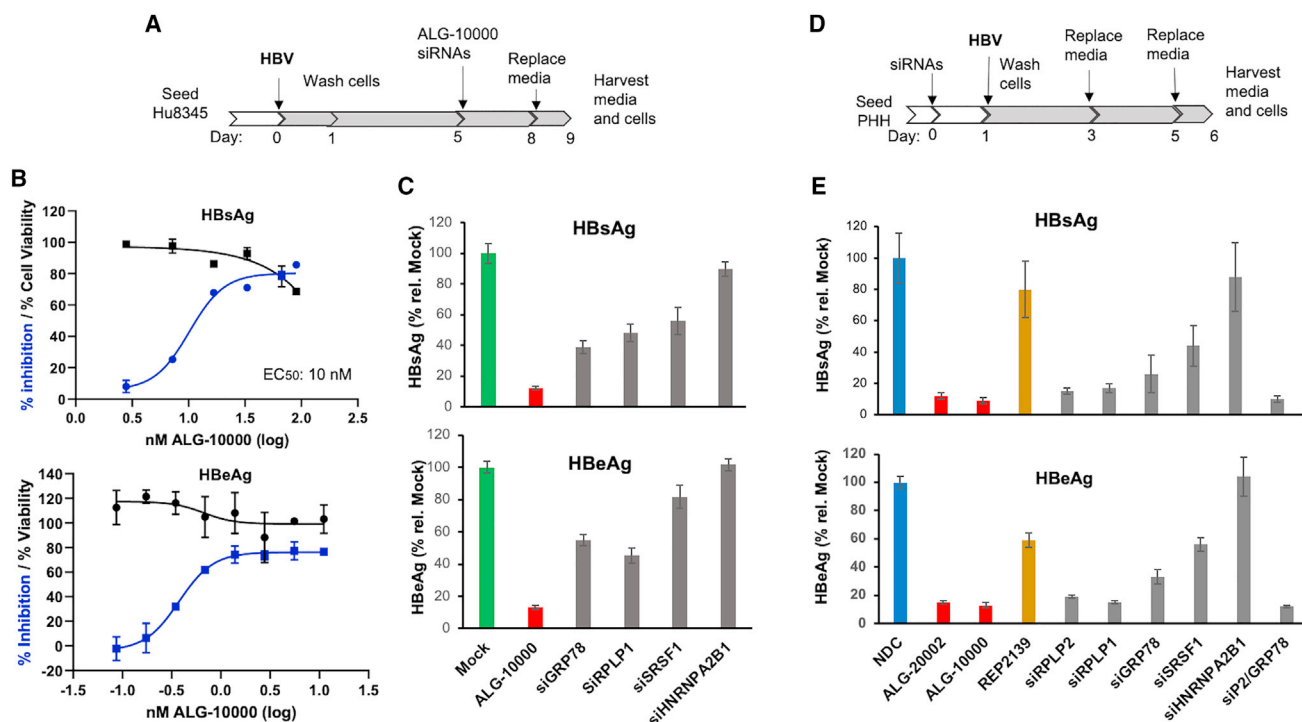
extracellular HBsAg and HBeAg levels (Figures 6C and S8). The knockdown of SRSF1 reduced HBsAg levels in HBV-infected PHHs but had a more modest effect on HBeAg (Figure 6C). Unexpectedly, the knockdown of HNRNP A2B1 did not reduce extracellular HBsAg and HBeAg made by the HBV-infected PHHs (Figure 6C). Western blot of the PHH cell lysates showed that HNRNP A2B1 was reduced by the siHNRNP A2B1, ruling out the possibility that the siRNA was not functional (Figure S8B).

Since STOPS sequester host factors, reducing the host factors before HBV infection should prophylactically decrease productive infection. To test this notion, PHHs were transfected with STOPS or siRNAs to knockdown the host factors prior to HBV infection (Figure 6D). PHHs transfected with ALG-10000 and ALG-20002 exhibited significantly reduced levels of extracellular HBsAg and HBeAg (Figure 6E). The knockdown of GRP78, RPLP1, RPLP2, and SRSF1 before HBV infection reduced extracellular HBsAg and HBeAg (Figure 6E). In

dose responses, the EC_{50} for HBsAg reduction was less than 1 nM (Figure S8C). REP 2139, which exhibited a higher EC_{50} in HepG2.2.15 cells, also exhibited a higher EC_{50} in HBV-infected PHHs. Again, the knockdown of HNRNP A2B1 did not affect extracellular HBsAg or HBeAg levels (Figure 6E). These results show that GRP78, RPLP1, RPLP2, and SRSF1 are important for HBV infection of PHH, while HNRNP A2B1 is not.

GRP78, RPLP1, and RPLP2 are required for the proper translation and folding of HBsAg

GRP78's involvement in HBsAg production suggests that STOPS affect protein folding and degradation. Ubiquitination and proteasome degradation are the major pathways to degrade mis-folded proteins.³³ Therefore, we examined whether STOPS could affect the ubiquitination of the HBsAg. The lysates from HepG2.2.15 cells transfected with ALG-10000 or siRNA were immunoprecipitated with antibody to HBsAg, eluted from the antibody, then subjected



to western blot analysis. The samples probed with an antibody to ubiquitin yielded a smear indicative of polyubiquitination (Figure S9). HBsAg ubiquitination in cells treated with ALG-10000 was approximately 2-fold higher than that of mock-treated samples (Figure S9). Immunoprecipitated samples probed with antibody to HBsAg showed a ladder of bands with a small increase in molecular weight (Figure 7A). Notably, HBsAg was already modified even in mock-treated cells but the ubiquitinated HBsAg increased in cells transfected with ALG-10000 or siRPLP2. These results show that HBsAg is normally ubiquitinated and that STOPS or a deficiency of RPLP2 can increase ubiquitination.

To better quantify HBsAg ubiquitination, we captured HBsAg from cell lysates on plates coated with anti-HBsAg antibody, and then detected ubiquitin with an antibody coupled to a reporter enzyme. The signal, normalized to the amount of intracellular HBsAg, demonstrated that ubiquitinated HBsAg increased by about 2-fold in ALG-10000-treated cells (Figure 7B). Ubiquitinated HBsAg was also increased by the knockdown of RPLP1, RPLP2, and GRP78, but not by the knockdown of SRSF1 (Figure 7C).

Proteasome inhibitors were used to examine whether STOPS affect the abundance of HBsAg through proteasome degradation. In cells treated with ALG-10000, proteasome inhibitors bortezomib or oprozomib did not affect extracellular HBsAg but resulted in a about 2-fold increase in the intracellular HBsAg (Figure 7D). Knockdown of siRPLP1 in HepG2.2.15 cells treated with bortezomib also increased intracellular HBsAg by more than 2-fold (Figure 7D). Finally, when the amounts of ubiquitinated intracellular HBsAg were increased in cells knocked down for RPLP1, RPLP2, and GRP78 and treated with bortezomib, the amount of ubiquitinated HBsAg was increased (Figure 7E). The knockdown of SFSR1, which likely does not directly function in HBsAg translation, did not increase the amount of ubiquitinated HBsAg. Altogether, RPLP1, RPLP2, and GRP78 participate in HBsAg production, and a reduction in their level in the cell resulted in increased ubiquitination and proteolysis of the HBsAg.

RPLP1 and RPLP2 require HBV RNA sequence to affect HBsAg production

Not all virus require RPLP1 or RPLP2 for the production of their structural proteins. We speculate that HBV may specifically recruit

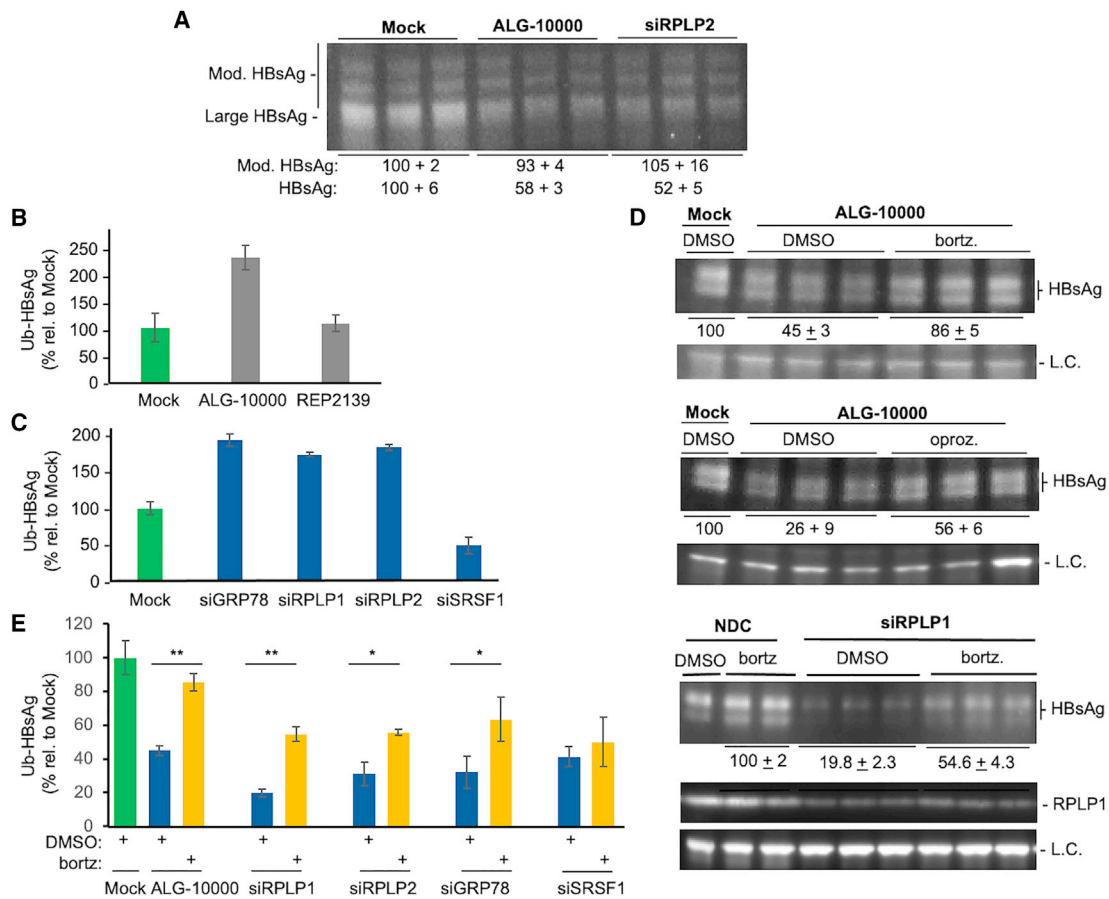


Figure 7. STOPS reduction of HBsAg involves ubiquitination of the HBsAg and proteasome degradation

(A) HBsAg has post-translational modifications. The HBsAg was from HepG2.2.15 cells treated with 8 nM ALG-10000 or 10 nM siRPLP2 for 76 h. The most prominent band is the molecular mass expected of the large HBsAg. Additional higher-molecular-weight bands may be ubiquitinated forms of the HBsAg. (B) Intracellular HBsAg in HepG2.2.15 cells treated with ALG-10000 increased the amount of ubiquitin. The ubiquitinated HBsAg assayed was from cells treated for 76 h with 8 nM ALG-10000. (C) Knockdown of GRP78, RPLP1, and RPLP2 can increase HBsAg ubiquitination. All siRNAs were transfected into HepG2.2.15 cells at a final concentration of 10 nM. The amount of ubiquitinated HBsAg was normalized to the amount of HBsAg present in the cell lysate. (D) Proteasome inhibitors can partially reverse ALG-10000-mediated reduction of HBsAg and RPLP1 levels. The images of the western blot show the large HBsAg in HepG2.2.15 transfected with 10 nM ALG-10000 and treated with the proteasome inhibitor bortezomib (25 nM), or oprozomib (100 nM), or DMSO, the vehicle used to solubilize the proteasome inhibitors. The cells were treated for 24 h before their lysis for western blot analysis. The LC is the protein GAPDH. siRPLP1 was transfected at 10 nM and the cells treated with bortezomib are as described in (A). (E) The amount of ubiquitinated HBsAg present in HepG2.2.15 cells after treatment with ALG-10000 or knockdown of GRP78, RPLP1, and RPLP2 is increased by treatment with the proteasome inhibitor bortezomib. * $p < 0.05$, ** $p < 0.01$. In the graphs in panels D, C, and E, each error bar represents one standard deviation of uncertainty.

these proteins to modulate the translation of the HBsAg.³⁴ To examine this possibility, the ORFs of the large and small HBsAg were cloned into the expression plasmid pCDNA3.1. In HEK 293 cells, both proteins were expressed. However, the knockdowns of the host factors did not reduce the amounts of small or large HBsAg (Figures 8A and S10A).

To determine whether additional HBV sequence(s) can enable the host factors to affect HBsAg production, a plasmid containing the 1.05X HBV genome, p1.05Gen_psiCHECK2, was tested. In 293 cells, HBsAg produced from this plasmid was sensitive to the knockdown of GRP78, RPLP1, and RPLP2 (Figure S10B). ALG-20002 that targets a sequence 3' of the HBsAg ORF also reduced HBsAg production, as

would be expected. Knockdown of SRSF1 did not affect HBsAg levels. These results suggest that additional sequences present in the HBV genome are required for GRP78, RPLP1 and RPLP2 to affect HBsAg production.

A series of constructs containing different HBV sequences cloned into expression plasmid pCDNA3.1 were made to map the sequence(s) required for host factor activity. HBsAg expressed from a sequence from the start of the polymerase ORF to the HBV 3' terminus in plasmid pPol-Gen_cDNA3.1 was sensitive to knockdown by RPLP1 and RPLP2 (Figure 8). Cells transfected with ALG-20002 also reduced the extracellular HBsAg expressed from this plasmid, as would be expected. HBsAg expressed from plasmid pPol-SAger_cDNA3.1,

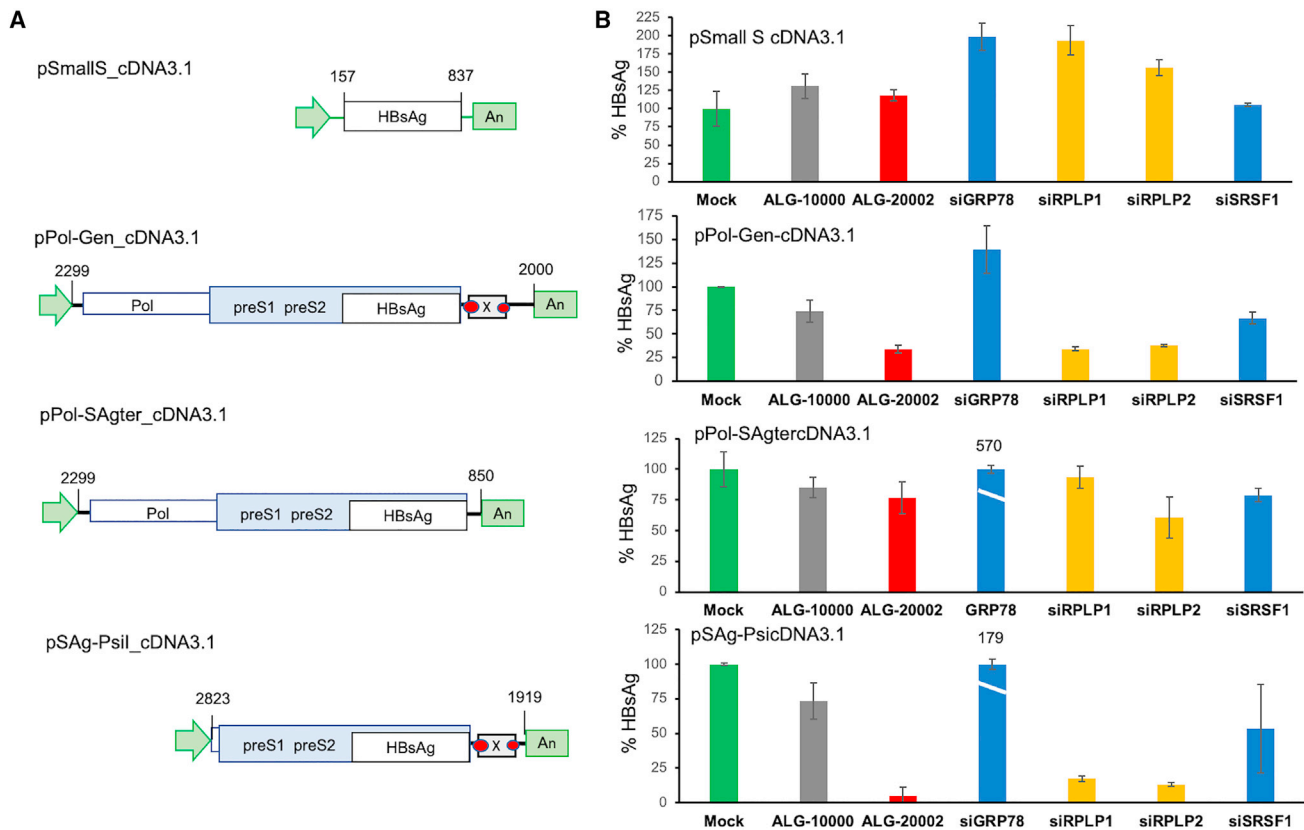


Figure 8. RPLP1 and RPLP2 require regulatory HBV sequences to function on HBsAg production

(A) Schematics of the HBV sequences cloned in plasmid pcDNA3.1 tested for HBsAg production. The nucleotide number of the HBV genome is shown at the flanks of the DNA sequence. The green arrow represents the human cytomegalovirus promoter. The green box labeled with “An” represents the polyadenylation sequence. Both the promoter and polyadenylation sequence are present in pcDNA3.1. Boxes represent the coding sequence for HBV genes. The two red ovals denote HBV enhancer sequences. (B) Relative amounts of the HBsAg produced in HEK 293 cells transfected with STOPS, siRNAs, or ALG-20002. HBsAg levels were reproducibly increased by the knockdown of GRP78 in cells transfected with pPol_SAgtercDNA3.1 and pSAg-PsicDNA3.1. The percentages of HBsAg expressed from these plasmids relative to the mock-treated control (pCDNA3.1) are shown above the blue bars. Each error bar represents one standard deviation of uncertainty.

which lacks the sequence 3' of the HBsAg ORF, was unaffected by the knockdown of RPLP1 and RPLP2 (Figure 8). Finally, HBsAg expressed from plasmid pSAg-Psil_cDNA3.1, which contains the HBsAg ORF and the HBV 3' sequence containing only a portion of the HBV epsilon sequence, was affected by the knockdown of RPLP1 and RPLP2 (Figure 8). These results suggest that sequence 3' of the HBsAg ORF, but not containing the intact epsilon element, contributes to engaging RPLP1 and RPLP2.

The knockdown of GRP78 reduced the amount of HBsAg produced from plasmid p1.05GEN_psiCHECK2, while its knockdown increased the amount of HBsAg produced from constructs that lack the sequence 5' of the polymerase ORF (Figures 8 and S10). GRP78 thus has a more complex role in HBsAg production that could involve some of its regulatory activities. These experiments show that the inhibition of HBsAg expression by STOPS is specific to HBV because sequences flanking the HBsAg ORF are required to engage RPLP1, RPLP2, and GRP78.

DISCUSSION

STOPS are a new class of NAPs that have the potential to dramatically reduce HBsAg in patients with chronic hepatitis. STOPS have significantly improved efficacy, being at least 20-fold more potent *in vitro* than previously described NAPs that could significantly reduce HBsAg in patient serum.^{16,17} Here, we have elucidated the mechanism of action of a prototype STOPS molecule, ALG-10000. ALG-10000 sequesters several cellular proteins needed to produce HBV proteins, including the HBsAg. Inadequate amounts of these cellular proteins resulted in reduced levels of HBsAg and increased the amounts of mis-folded protein that was degraded by the proteasome.

The chemical features of the STOPS molecules allow them to reduce HBV infection. Phosphorothioated oligonucleotides have higher affinities for the bound proteins than their phosphodiester counterparts.³⁵ High-affinity binding by STOPS could render the bound proteins in conformations susceptible to being degraded. Host factors bound by ALG-10000 are present in reduced amounts, probably due

to increased degradation. Reducing the amounts of the host proteins for molecular synthesis takes time and may account for the slow kinetics for HBsAg reduction. The AC repeats of STOPS contributes to the recognition by RNA-binding host proteins. Although SRSF1 and HNRNPA2B1 recognize a sequence containing the splice junction motif, they could also preferentially bind RNAs containing CA dinucleotide motifs.^{36,37} Finally, the 40-nt length of STOPS molecules may allow contact with multiple proteins. ALG-10000 lacks inter- or intramolecular base-pairing interactions, perhaps due to the methylene linkage between the ribose 2' oxygen and 4' carbon. While oligonucleotides containing LNAs strengthen binding to nucleic acid targets,³⁸ STOPS like ALG-10000 may be too conformationally stiff to form intramolecular base pairs, or base pair with another ALG-10000 molecule. All of the chemical features of STOPS appear to contribute to their mechanism of action.

STOPS binding to multiple host proteins accounts for the inhibition of HBV infection and HBsAg production. SRSF1 and HNRNPA2B1 function in RNA processing and RNA metabolism. STOPS and the host factor knockdown will reduce the total amounts of HBV only by up to 2-fold, suggesting that SRSF1 and HNRNPA2B1 may only act on select HBV RNAs. Consistent with this is that knockdown of SRSF1 and HNRNPA2B1 dramatically reduced HBsAg levels in HepG2.2.15 cells but only minimally reduced the HBeAg. It should be noted that HNRNPA2B1 is not needed for all cells infected by HBV. HNRNPA2B1 is a member of a family of proteins that can functionally complement each other.³⁹ HNRNPA2B1 also recognizes m6A-modified RNA, and the m6A modification could vary with cells.²⁴

The major effect of STOPS on HBV infection was at the level of protein production and degradation. Viral structural proteins are typically made at high levels and may have additional requirements to their production, such as specialized translational factors and/or protein chaperones.⁴⁰ For dengue virus, RPLP1/2 decreases the time for translational pausing that could be evolved to coordinate polypeptide synthesis and modification/processing.^{22,41} A reduction in the amounts of RPLP1/2 could alter the proper timing needed to produce, fold, and post-translationally modify HBsAg. Reduced amounts of GRP78 could result in increased amounts of mis-folded or improperly modified HBsAg that are subject to degradation. RPLP1 and RPLP2 are also required for the normal amounts of HBeAg and HBV polymerase. HBeAg has a signal peptide and is secreted after proteolytic processing, and it seems likely that RPLP1/2 and GRP78 are needed for its production and secretion. The HBV polymerase, however, is not a transmembrane protein. We speculate that RPLP1/2 and GRP78 may not be restricted to acting on transmembrane proteins.

Viruses are the masters of co-opting cellular factors for their own advantage. For the translation and production of HBsAg, HBV possesses additional RNA sequences to engage RPLP1/2 and GRP78. To our knowledge, RPLP1/2 and GRP78 have not been described to specifically bind RNA. Martinez-Azorin et al.⁴¹ have previously

shown that RPLP1 and RPLP2 act to translate foot-and-mouth disease virus proteins that are made by internal ribosomal entry, but they did not demonstrate that RPLP1 and RPLP2 bind RNA. We cannot rule out that an accessory protein that binds RNA may bridge the contact between the HBV RNA and host factors GRP78 and RPLP1/2.

Antiviral compounds that act on cellular proteins have the advantage of decreasing the chance of the emergence of viral resistant mutations. However, a concern for molecules that act on cellular targets will be that they will demonstrate toxicity. We have not observed that effective concentrations of STOPS will cause toxicity *in vitro*. Approved antivirals that act on cellular targets include maraviroc and the nucleotide analogue cytarabine.⁴² Modified oligonucleotides that target host molecules have also been approved to treat liver diseases or to reduce proteins made by the liver.^{43,44} The technology to preferentially target oligonucleotides to the liver, the site for HBV infection, is relatively mature.⁴⁵ STOPS inhibition of HBsAg and HBeAg production and acceleration of HBsAg degradation could contribute to the functional cure of CHB.

MATERIALS AND METHODS

Key reagents

Deoxynivalenol (catalog # D0156) and cyanogen bromide-activated sepharose (catalog # S9142-1) are from Sigma-Aldrich. Bortezomib (catalog # ab142123) is from Abcam, and oprozomib (catalog # S7049) is from SelleckChem.

siRNAs that targeted host proteins were from the OnTARGETplus series from Horizon Discovery: siGRP78 (catalog # L-1008198-01), siRPLP1 (catalog # L-011135-00), siRPLP2 (catalog # L-004314-01), siSRSF1 (catalog # L-018672-01), siHNRNPA2B1 (L-011690-01), siDNAJB9 (catalog # L-012815-00), and siDNAJB12 (catalog # L-020585-00).

The majority of primary antibodies and horseradish peroxidase-conjugated secondary antibodies were from Abcam: anti-GRP78 (catalog # ab191023), anti-RPLP1 (catalog # ab121190), anti-RPLP2 (catalog # ab154958), anti-HNRNPA2B1 (catalog # ab6102), anti- β -actin (catalog # ab8227), anti-GAPDH (catalog # ab8245), goat anti-rabbit-HRP (catalog # ab6721), and goat anti-mouse-HRP (catalog # ab6789). Anti-SRSF1 is from Invitrogen (catalog # 32-4600). Anti-HBsAg is from Fitzgerald Industries (catalog # 20-HR20). Anti-HBV polymerase is from Santa Cruz Biotech (catalog # Sc-81590). Anti-ubiquitin-HRP P4D1 is from Cytoskeleton (catalog # 140495).

Chemical synthesis of STOPS

Oligonucleotides, including STOPS, were synthesized on an ABI394 DNA synthesizer at 1- μ mol scale using universal linker solid support. The synthesized material was deprotected and cleaved from the solid support by heating at 55°C in an ammonium hydroxide solution overnight or 65°C in a 1:1 ammonium hydroxide/methyl amine solution for 90 min. The reaction mixtures were filtered and evaporated in a Savant SpeedVac. The residues were reconstituted in water and

purified using an ion exchange high-pressure liquid chromatography (HPLC) column (Thermo Scientific DNAPac PA-100, 9 × 250 mm) in a gradient of 25%–85% buffer B amended to buffer A (buffer A was 20 mM sodium phosphate, 10% acetonitrile in water, pH 8; buffer B was 20 mM sodium phosphate, 1.8 M sodium bromide, 10% acetonitrile in water, pH 8). The purified material was dried, reconstituted in water, desalted using Sephadex-25 columns, and eluted with DNase/RNase-free distilled water. The final samples were characterized by analyzing the sample mass and purity using liquid chromatography-mass spectrometry (LC-MS) and reversed-phase HPLC. The final solutions were quantified by measuring absorbance at 260 nm using NanoDrop 2000c.

Thermodenaturation studies

All samples were prepared at 2 μM concentration in Corning phosphate-buffered saline (PBS; catalog # 21-040-CV Corning). Where present, PBS was amended to contain 1 M NaCl, or 1 M NaCl and 2.5 mM MgCl₂. The data were collected using a Shimadzu UV2600 spectrophotometer connected to a TMSPC-8 unit and recorded at a rate of 1°C/min, in 1°C intervals, for both the heating (20°C–95°C) and cooling (95°C–20°C) runs. Three independent trials were conducted for each molecule.

Cell cultures and manipulations

HepG2.2.15 cells that contain integrated tandem HBV genome and constitutively express HBsAg were grown and manipulated in a DMEM/F12 (1:1) media (catalog # 2021-05, Corning) containing 10% fetal bovine serum (FBS) (catalog # F8192; Sigma), 1× nonessential amino acids (catalog # 34319012, Corning), and 1% penicillin and streptomycin (catalog # 30-002, Corning). All manipulations used cells grown on collagen-coated 96-well plates cultured at 37°C with 5% CO₂.

HepG2-NTCP cells were maintained in DMEM/F12 (catalog # 10-092-CM, Corning) with 10% FBS, 1% penicillin and streptomycin, 2 mM glutamine, 1% nonessential amino acids, and 1% sodium pyruvate. The cells were seeded at 20,000 cells/well in a 96-well plate. After the cells attached overnight, they were infected with HBV with 200 genome equivalents of HBV AD38 (genotype D; strain AYW). The infected cells were transfected with STOPS using Lipofectamine RNAiMAX on days 5 and 8. The HBsAg was measured in the supernatant on day 11, and the remaining cells were measured for cell viability. HBsAg was measured with an ELISA kit, and cell viability was measured with the CellTiter-Glo (catalog # G7573, Promega) assay kit according to the manufacturer's instructions.

PHHs were obtained as frozen vials from BioIVT. The cells were thawed, transferred to a 15-mL conical tube with 10 mL of plating medium (Life Technologies). The cells were gently pelleted at 70 g for 5 min and resuspended in plating medium at 5.0 × 10⁵ cells/mL, then 0.1 mL of this was plated into each well of a collagen-coated 96-well plate. HBV infection was carried out in the PHH culturing medium (DMEM + 10% FBS, 1× penicillin/streptomycin, 20 mM

HEPES, 0.1 mM ascorbic acid 2-phosphate, 15 mg/mL L-proline, 0.25 mg/mL insulin, 5 ng/mL epidermal growth factor, and 50 nM dexamethasone) containing 2% DMSO, 4% PEG8000, and virus at 200 genome equivalents of virus/well. After a 24-h incubation at 37°C, the infected cells were washed thrice with a washing medium (DMEM + 2% FBS, 1× penicillin/streptomycin, and 20 mM HEPES) and restored in the culturing medium. The medium was replenished every 3 days during the infection. The PHHs were transfected in 96-well collagen-coated plates with oligonucleotides using 0.3 μL/well of Lipofectamine RNAiMax.

HEK 293 cells were grown and manipulated in minimal essential medium (MEM) medium supplemented with 10% FBS, 1× nonessential amino acids, and 1× penicillin/streptomycin. The cells were typically plated at 40,000 cells per well into a 96-well plate.

Oligonucleotide and plasmid transfection

Each oligonucleotide to be transfected was diluted in Opti-MEM (catalog # 31980-070, Gibco) with 0.3 μL of Lipofectamine RNAiMax (catalog # 13778-500, Invitrogen). HepG2.2.15 cells were typically transfected while the cells were plated. HepG2-NTCP and PHHs were transfected after the cells were attached to the plates. Plasmids were directly transfected into cells at a ratio of 100 ng/well and 0.3 μL of Lipofectamine 2000 (catalog # 11668-019, Invitrogen).

Protein detection and quantification

Extracellular HBV HBsAg and HBeAg were quantified using ELISA kits (catalog # DS187701 and catalog # 05187703, DiaSino). The amounts of signal for HBsAg and HBeAg were assessed by chemiluminescence. HBV core protein was quantified using a colorimetric ELISA assay (catalog # VPK-150, Cell Biolabs). Chemiluminescence and color change was quantified using the Envision 2102 multi-label plate reader.

Western blots used cells that were lysed with ice-cold cell lysis buffer (catalog # 87787, Pierce) containing protease inhibitors (catalog # 04-693-132-001, Roche). The lysates used to quantify the amount of ubiquitination were modified with deubiquitinase inhibitors (catalog # NEM09BB, Cytoskeleton) according to the manufacturer's instructions. The lysate was then treated with universal nuclease (catalog # 88700, Pierce) for 10 min to decrease their viscosity. Denaturing Laemmli loading buffer containing β-mercaptoethanol to 2 mM was added to a final concentration of 1×, and the lysate was incubated for 5 min at 85°C. Molecules in the lysate were separated by electrophoresis in 4%–12% NuPAGE Bis-Tris gel (catalog # NP0336, Invitrogen), followed by transfer to membranes and incubation with the primary and secondary antibodies. The western blot blocking and washes were performed with PBS-Tween 20 (catalog # 28352, Thermo Fisher). Western blot signals were developed with chemiluminescence substrate solution (catalog # 34579, Thermo Fisher) and imaged with a ProteinSimple imager. Quantification of the bands from the acquired images was performed using ImageJ software.

The HBsAg ELISA assay was adapted to quantify the ubiquitins attached to HBsAg. Lysates from the HepG2.2.15 cells were prepared in the lysis buffer containing both protease inhibitors and deubiquitinase inhibitors, and 30 μ L of the lysate was diluted in Opti-MEM to a 100- μ L volume that was then incubated with gentle shaking for 1 h at room temperature on an HBsAg capture plate. The plate was then washed five times with 250 μ L of a wash buffer and incubated with a solution of anti-ubiquitin antibody conjugated to horseradish peroxidase for 1 h at room temperature. Following another 1-h incubation with gentle shaking at room temperature, the plate was washed five times and incubated with chemiluminescence substrate. The signal was quantified with an Envision 2102 multi-label plate reader.

RNA quantification

HBV RNA quantification used the QuantiGene assay kit (Thermo Fisher catalog # QS0009) according to the manufacturer's instructions. Briefly, cells were washed with cold PBS once, then lysed with the QuantiGene lysis buffer containing protease K (Thermo Fisher, catalog # QS0512) at 37°C for 30 min. Twenty microliters of the cell lysate was used for hybridization with HBV RNA probe which targets the Hepatitis B Protein X (HBX) coding region (Thermo Fisher, catalog #SF-10405) for signal normalization. After an overnight hybridization on the capture plates, excess probes were washed away and the hybridization signal was amplified by hybridization with pre-amplifier, amplifier probe, and labeling probe. The chemiluminescence readout was determined using the Envision 2102 multi-label plate reader.

Quantification of the knockdown of siRNAs used real-time qRT-PCR. Total RNA was extracted from cells using the QuickExtract RNA extraction kit (catalog # QER090150, Lucigen) according to the manufacturer's instructions. The cells were washed with cold PBS and lysed with RNA extraction solution by vortexing for 1 min, then centrifuged. The lysate was incubated at 65°C for 2 min, then treated with DNase at 37°C for 15 min, followed by incubation with the stop solution at 65°C for 10 min. RNA was quantified by qRT-PCR using qScript XLT One-Step RT-qPCR ToughMix (Quantabio, catalog #95132-500) and GRP78, RPLP1, RPLP2, or 18S TaqMan Gene Expression assays (catalog # 4448490). Two microliters of cell lysate was added to 20 μ L of the reaction mix. qRT-PCR was performed on a qTower platform (Analytic-Jena) at 50°C for 10 min for reverse transcription, then 95°C for 1 min. DNA amplification used 40 cycles at 95°C for 10 s followed by 60°C for 45 s.

Confocal microscopy

HepG2.2.15 cells were grown on poly-L-lysine-coated coverslips to 60% confluency. After transfection, the cells were cultured for 24 h and then were fixed with 4% paraformaldehyde for 15 min at room temperature. The cells were washed with PBS twice and mounted on glass slides with anti-fade mounting medium and DAPI (catalog # P36941, Life Technologies), then dried overnight in the dark. Micrographs were acquired with a Leica TCS SP5 confocal inverted-base microscope with a 63 \times oil objective. The images were processed

with the Leica LAS AF and ImageJ software. Colocalization of fluorophores was quantified using an ImageJ plug-in tool JACoP.⁴⁶

Proteomic analysis

The ALG-10000 affinity resin was made using the standard protocol suggested by the manufacturer of the CNBr-activated Sepharose resin (Sigma). Unreacted groups on the resin were quenched with 0.1 M Tris-Cl. A control resin used Tris-Cl as the ligand. After extensive washing in high salt, the resin that reacted with ALG-10000 contained over 125-fold more nucleic acid than the control resin.

The ALG-10000 resin and Tris resin were incubated with extracts from HepG2.2.15 cells solubilized by Dounce homogenization in a Tris-buffered saline containing 0.05% Tween 20 and protease inhibitors (catalog # 11873580001, Roche) for 1 h. The resin was then washed four times with the extraction buffer that contained increasing salt concentrations up to 1 M followed by a final wash with Tris-buffered saline. The resin and associated proteins were treated with trypsin (catalog # V5280, Promega) overnight, followed by termination of the reaction with 10% trifluoroacetic acid. Peptides were then purified using C-18 reverse-phase Zip-Tips (catalog # ZTC18S096, EMD Millipore) and subjected to LC-MS/MS. Peptide quantification was performed by summation of the peptide ion intensities after normalization to the signal from the bradykinin fragment. Peptides were resolved by a Bruker Autoflex III MALDI-ToF mass spectrometer (Agilent Technologies) in positive ion mode. Assigned peaks all corresponded to within 0.5 Da of their theoretical masses. Database searches used the program Mascot (Matrix Science), with searches directed against the NCBI's human proteome and viral proteomes.

Expression of recombinant HBsAg

The sequence of the HBV genotype D (GeneBank: NC003977.2) was used for cloning. The sequence used was numbered from 1 to 3,182; however, it should be noted that the HBV genome is circular and terminally redundant, and that cloning of HBV sequences for protein expression may span more than one genome. For the small S, the sequence from nucleotide 157 to 837 was chemically synthesized with flanking NheI and NotI sites and cloned into the same restriction sites in pCDNA3.1. cDNA to express the large S antigen was from nucleotide 2,850 to 837, flanked by the NheI and NotI sites, and was cloned into pCDNA3.1. This sequence has the initiation codon for the middle and small S antigens mutated from ATG to AGG to ensure that only the large S antigen was translated. The 1.05X genome of HBV with a duplicated terminal sequence was chemically synthesized from nucleotide 1,808 to 2,000 flanked with SalI and NotI restriction sites. This was cloned into the XhoI and NotI restriction sites of the plasmid psiCHECK2.

DNAs to generate pPol-Gen-cDNA3.1 and pSag-Gen_cDNA were chemically synthesized with flanking NheI and ApaI restriction sites. The insert was digested with restriction enzymes and ligated to pCDNA3.1 that had been cleaved with NheI and ApaI. The DNA to generate pSag-PsiI_cDNA3.1 was generated from a

chemically synthesized DNA that contained an NheI site 5' of the large HBsAg ORF to the 3' termini of the HBV genome. The DNA was cleaved with the NheI restriction enzyme and a PsiI restriction enzyme that cleaves at nt 1,919 of the HBV genome. The cleaved DNA was ligated to pcDNA3.1, which had been cleaved with restriction enzymes NheI and EcoRV. Plasmids for transfection were prepared using the EndoFree Plasmid Maxiprep kit (catalog # 12362; Qiagen).

HEK 293 cells were seeded in 96-well plates at 4×10^5 cells per well. After attachment, the cells were transfected with oligonucleotides (10 nM ALG-10000, 5 nM ALG-20002, and 10 nM siRNA) and, 48 h later, super-transfected with 100 ng/well of plasmids encoding the HBsAg. The cell culture medium was harvested at 36 h post plasmid transfection to quantify the HBsAg by ELISA. Cell lysates were also collected at that time to examine the abundance of the cellular proteins.

SUPPLEMENTAL INFORMATION

Supplemental information can be found online at <https://doi.org/10.1016/j.omtn.2021.12.013>.

ACKNOWLEDGMENTS

We thank Robert Vaughan for mass spectrometric analyses and Guanghui Yi for confocal microscopy. We thank Michelle Burke for generating a model for the mechanism of action of STOPS and Laura Kao for editing.

AUTHOR CONTRIBUTIONS

C.C.K. was responsible for the majority of the results in the manuscript and was primarily responsible for the writing of the manuscript. J.A.S. and L.B. provided critical guidance, editing, and approval of the work in the manuscript. Y.N. contributed the results in Figures 1B and 1C and generated two of the constructs used in Figure 8. S.R. contributed to the results in Figures 2F, 5F, and S7. T.S.D.C. contributed Figure 4A and synthesized the molecules tested in Figure 4B. S.R. and T.S.D.C. contributed to the editing of the manuscript. L.B., R.K.P., J.H., D.B.S., and L.B. established the design, chemical synthesis of the oligonucleotides, and their analytical and functional analyses. D.B.S. also edited the manuscript. L.M.B. conceived the project and provided critical analyses and resources for the project.

DECLARATION OF INTERESTS

All authors declare no competing interests.

REFERENCES

- World Health Organization (2021). Global Progress Report on HIV, Viral Hepatitis and Sexually Transmitted Infections (World Health Organization), ISBN: 978-92-4-002707-7.
- Tang, L.S.Y., Covert, E., Wilson, E., and Kottlilil, S. (2018). Chronic hepatitis B infection, a review. *JAMA* 319:1802-1813.6. Yip TC, Lok AS. 2020. How do we determine whether a functional cure of HBV infection has been achieved? *Clin. Gastroenterol. Hepatol.* 18, 548-550.
- Faure-Dupuy, S., Lucifora, J., and Durantel, D. (2017). Interplay between the hepatitis B virus and innate immunity: from an understanding to the development of therapeutic concepts. *Viruses* 9, 95.
- Tan, A., Koh, S., and Bertoletti, A. (2015). Immune response in hepatitis B virus infection. *Cold Spring Harb Perspect. Med.* 5, a021428.
- Kim, W.R. (2018). Emerging therapies toward a functional cure for hepatitis B virus infection. *Gastroenterol. Hepatol.* 14, 439-442.
- Liang, T.J., Block, T.M., McMahon, B.J., Ghany, M.G., Urban, S., Guo, J.-T., Locarnini, S., Zoulim, F., Chang, K.-M., and Lok, A.S. (2015). Present and future therapies of hepatitis B: from discovery to cure. *Hepatol.* 62, 1893-1908.
- Ahn, S.H., Park, Y.N., Park, J.Y., Chang, H.-Y., Lee, J.M., Shin, J.E., Han, K.-H., Park, C., Moon, Y.M., and Chon, C.Y. (2005). Long-term clinical and histological outcomes in patients with spontaneous hepatitis B surface antigen seroclearance. *J. Hepatol.* 42, 188-194.
- Alawad, A.S., Auh, S., Suarez, D., and Ghany, M.G. (2020). Durability of spontaneous and treatment-related loss of hepatitis B S-antigen. *Clin. Gastroenterol Hepatol.* 18, 700-709.e3.
- Yuen, M.F., Wong, D.K.-H., Fung, J., Ip, P., But, D., Hung, I., Lau, K., Yuen, J.C.-H., and Lai, C.-L. (2008). HBsAg seroclearance in chronic hepatitis B in Asian patients: replicative level and risk of hepatocellular carcinoma. *Gastroenterology* 135, 1192-1199.
- Tout I, Loureiro D, Mansour A, Soumelis V, Boyer N, and Asselah T. Hepatitis B surface antigen seroclearance: immune mechanisms, clinical impact, importance for drug development. *J. Hepatol.* 73: 409-422.
- Yip, T.C., Wong, G.L., Chan, H.L., Tse, Y.K., Lam, K.L., Lui, G.C., and Wong, V.W. (2019). HBsAg seroclearance further reduces hepatocellular carcinoma risk after complete viral suppression with nucleos(t)ide analogues. *J. Hepatol.* 70, 361-370.
- Asselah, T., Loureiro, D., Boyer, N., and Mansouri, A. (2019). Targets and future direct-acting antiviral approaches to achieve hepatitis B virus cure. *Lancet Gastroenterol. Hepatol.* 4, 883-892.
- Noordeen, F., Vaillant, A., and Jilbert, A.R. (2013). Nucleic acid polymers inhibit duck hepatitis B virus infection *in vitro*. *Antimicrob. Agents Chemother.* 57, 5291-5298.
- Noordeen, F., Vaillant, A., and Jilbert, A.R. (2013). Nucleic acid polymers prevent the establishment of duck hepatitis B virus infection *in vivo*. *Antimicrob. Agents Chemother.* 57, 5299-5308.
- Quinet, J., Jamard, C., Burtin, M., Lemasson, M., Guerret, S., Sureau, C., Vaillant, A., and Cova, L. (2018). Nucleic acid polymerase REP 2139 and nucleos(T)ide analogues act synergistically against chronic hepadnaviral infection *in vitro* in Pekin ducks. *Hepatology* 67, 2127-2140.
- Al-Mahtab, M., Bazinet, M., and Vaillant, A. (2016). Safety and efficacy of nucleic acid polymers in monotherapy and combined with immunotherapy in treatment-naïve Bangladeshi patients with HBeAg+ chronic hepatitis B infection. *PLoS One* 11, e0156667.
- Bazinet, M., Pantea, V., Cebotarescu, V., Cojuhari, L., Albrecht, J., Schmid, P., Le Gal, F., Gordien, E., Krawczyk, A., Mijocovic, H., et al. (2017). Safety and efficacy of REP 2130 and pegylated interferon alfa-2a for treatment-naïve patients with chronic hepatitis B virus and hepatitis D virus co-infection (REP 301 and REP 301-LTF): a non-randomised, open-label, phase 2 trial. *Lancet Gastroenterol. Hepatol.* 2, 877-889.
- Real, C.L., Werner, M., Paul, A., Gerken, G., Schlaak, J.F., Vaillant, A., and Broering, R. (2017). Nucleic acid-based polymers effective against hepatitis B virus infection in patients don't harbor immunostimulatory properties in primary isolated liver cells. *Sci. Rep.* 7, 43838.
- Beilstein, F., Blanchet, M., Vaillant, A., and Sureau, C. (2018). Nucleic acid polymers are active against hepatitis delta virus infection *in vitro*. *J. Virol.* 92, e01416-e01417.
- Fitzgerald, M., Hong, J., Pandey, R., Rajwanshi, V., Hua, T., Nie, Y., Kao, C., Ren, S., Cortez, J., Smith, D., et al. (2020). Structural requirements for S-antigen transport-inhibiting oligonucleotide polymer inhibition of hepatitis B surface antigen secretion. *J. Hepatol.* 73, S876-S877.
- Boulon, R., Blanchet, M., Lemasson, M., Vaillant, A., and Labonté, P. (2020). Characterization of the antiviral effects of REP 2139 on the HBV lifecycle *in vitro*. *Antiviral Res* 183, 104853.

22. Campos, R.K., Wijeratne, H.R.S., Shah, P., Garcia-Blanco, M.A., and Bradrick, S.S. (2020). Ribosomal stalk proteins RPLP1 and RPLP2 promote biogenesis of flaviviral and cellular multi-pass transmembrane proteins. *Nucleic Acids Res.* *48*, 9872–9885.
23. Wang, M., Way, S., Zhang, Y., Ye, R., and Lee, A.S. (2009). Role of the unfolded protein response regulator GRP78/BiP in development, cancer, and neurological disorders. *Antioxid. Redox Signal.* *11*, 2307–2316.
24. Wu, B., Su, S., Patil, D.P., Liu, H., Gan, J., Jaffrey, S.R., and Ma, J. (2018). Molecular basis for the specific and multivalent recognitions of RNA substrates by human hnRNP2B1. *Nat. Commun.* *9*, 420.
25. Das, S., and Krainer, A.R. (2014). Emerging functions of SRSF1, splicing protein and oncoprotein, in RNA metabolism and cancer. *Mol. Cancer Res.* *12*, 1195–1204.
26. Campos, R.K., Wong, B., Xie, X., Lu, Y.F., Shi, P.Y., Pompon, J., Garcia-Blanco, M.A., and Bradrick, S. (2017). RPLP1 and RPLP2 are essential flavivirus host factors that promote early viral protein accumulation. *J. Virol.* *91*, e01706–e01716.
27. Choukhi, A., Ung, S., Wychowski, C., and Dubuisson, J. (1998). Involvement of endoplasmic reticulum chaperones in the folding of hepatitis C virus glycoproteins. *J. Virol.* *72*, 3851–3858.
28. Nain, M., Mukherjee, S., Karmakar, S.P., Paton, A.W., Paton, J.W., Abdin, M.Z., Basu, A., Kalia, M., and Vrati, S. (2017). GRP78 is an important host factor for Japanese encephalitis virus replication in mammalian cells. *J. Virol.* *91*, e02274–16.
29. Paz, S., Krainer, A.R., and Caputi, M. (2014). HIV-1 transcription is regulated by splicing factor SRSF1. *Nucleic Acids Res.* *42*, 13812–13823.
30. Zhou, X., Wang, L., Zou, W., Chen, X., Roizman, B., and Zhou, G.G. (2020). hnRNP2B1 associated with recruitment of RNA into exosomes plays a key role in herpes simplex virus 1 release from infected cells. *J. Virol.* *94*, e00367–20.
31. Liljas, A., and Sanyal, S. (2018). The enigmatic ribosomal stalk. *Q. Rev. Biophys.* *51*, e12.1–12.
32. Cléry, A., Sinha, R., Anczuków, O., Corrionero, A., Moursy, A., Daubner, G.M., Valcarcel, J., Krainer, A., and Allain, F.H. (2013). Isolated pseudo-RNA recognition motifs of SR proteins can regulate splicing using a noncanonical mode of RNA recognition. *Proc. Natl. Acad. Sci. U S A* *110*, E2802–E2811.
33. Pohl, C., and Dikic, I. (2019). Cellular quality control by the ubiquitin-proteasome system and autophagy. *Science* *366*, 812–822.
34. Spurger, K.B., Alefantis, T., Peyser, B.D., Ruthel, G.T., Bergeron, A.A., Costantino, J.A., Enterlein, S., Kota, K.P., Boltz, R.C.D., Aman, M.J., et al. (2010). Identification of essential filovirion-associated host factors by serial proteomic analysis and RNAi screen. *Mol. Cell Proteomics* *9*, 2690–2703.
35. Hyjek-Skladanowska, M.H., Vickers, T.A., Napiorkowska, A., Anderson, B.A., Tanowitz, M., Crooke, S.T., Seth, P.P., and Nowotny, M. (2020). Origins of the increased affinity of phosphorothioate-modified therapeutic nucleic acids for proteins. *J. Am. Chem. Soc.* *142*, 7456–7468.
36. Cléry, A., Krepl, M., Nguyen, C.K.X., Moursy, A., Jorjani, H., Katsantoni, M., Okoniewski, M., Mittal, N., Zavalan, M., Sponer, J., et al. (2021). Structure of SRSF1 RRM1 bound to RNA reveals an unexpected bimodal mode of interaction and explains its involvement in SMN1 exon 7 splicing. *Nat. Commun.* *12*, 428.
37. Schreiner, S., Didio, A., Hu, L.-H., and Bindereif, A. (2020). Design and applications of circular RNAs with protein-sponge function. *Nucleic Acids Res.* *48*, 12326–12335.
38. Braasch, D.A., and Corey, D.R. (2001). Locked nucleic acid (LNA): fine-tuning the recognition of DNA and RNA. *Chem. Biol.* *8*, 1–7.
39. Guereens, T., Bouhy, D., and Timmerman, V. (2016). The hnRNP family: insights into their role in health and disease. *Hum. Genet.* *135*, 851–867.
40. Li, S. (2019). Regulation of ribosomal proteins on viral infection. *Cells* *8*, 508.
41. Martinez-Azorin, F., Remacha, M., Martinez-Salas, E., and Ballesta, J.P. (2008). Internal translation initiation on the foot-and-mouth disease virus IRES is affected by ribosomal stalk conformation. *FEBS Lett.* *582*, 3029–3032.
42. Woollard, S.M., and Kanmogne, G.D. (2015). Maraviroc: a review of its use in HIV infection and beyond. *Drug Des Devel Ther* *9*, 5447–5468.
43. Adams, D., Gonzalez-Duarte, A., O’Riordan, W.D., Yang, C.C., Ueda, M., Tourneval, I., Schmidt, H.H., Brannagan, T.H., Kim, B.J., Oh, J., et al. (2018). Patisiran, and RNAi therapeutic, for hereditary transthyretin amyloidosis. *N. Engl. J. Med.* *379*, 11–21.
44. Honor, A., Rudnick, S.R., and Bonkovsky, H.L. (2021). Givosiran to treat porphyria. *Drugs Today* *57*, 47–59.
45. Debacker, A.J., Voutilainen, J., Catley, M., and Habib, N. (2020). Delivery of oligonucleotides to the liver with GalNAc: from research to registered therapeutic drugs. *Mol. Ther.* *28*, 1759–1771.
46. Bolte, S., and Cordelieres, F.P. (2006). A guided tour into subcellular colocalization analysis in light microscopy. *J. Microsc.* *224*, 213–232.